POST-ERUPTION LAVA DOME EMPLACEMENT MEASURED BY UAV PHOTOGRAMMETRY: AN INVESTIGATION ONE YEAR AFTER THE 2017-2019 MT. AGUNG ERUPTIONS

Ruli Andaru* [1,2], Jiann-Yeou Rau [2], Devy Kamil Syahbana [3], Heruningtyas Desi Purnamasari[3]

[1] Department of Geodetic Engineering, Gadjah Mada University, Indonesia– ruliandaru@ugm.ac.id
[2] Department of Geomatics, National Cheng Kung University, Taiwan
[3] Center for Volcanology and Geological Hazard Mitigation, Geological Agency,
Ministry of Energy and Mineral Resources, Indonesia

Commission II, WG II/5

KEYWORDS: Lava Dome Emplacement, Post-Eruption, UAV Photogrammetry, Mount Agung

ABSTRACT:

We present an observation of morphological changes at Mt. Agung lava dome one year after the 2017–2019 eruption crisis using UAV-photogrammetry method. Five time-series UAV datasets involve the images collected during the crisis period and the newest data collection (July 16, 2020) were used to provide a detailed investigation of the changes in morphology inside the crater and land cover on the surrounding slopes. The digital surface models (DSMs) generated by structure-from-motion (SfM) with multi-view stereo (MVS) algorithm were used to quantify the dome growth, the surface emplacement, and the actual remaining deposited material eruption surrounding the summit. Analysis of the last two series orthoimages indicates that the crater surface's texture remarkably unchanged one year after the eruption crisis (the dome still presents rough surfaces that resemble small stones and sand). According to the DSMs difference, it is evident that there were no considerable surface displacements inside the dome. It implies that no significant magma pressure accumulation occurring the dome. However, we found a small-scale growth in the central dome, which has increased the dome height up to 2 m and inflate the dome with a volume of 45,950 m^3. We have also observed a new lava lake (e.g., compound lava) with an area of 9,166 m^2 in the southeast of the dome edge. This new lava lake uplifts the surface up to 29 m and translated to a 79,623 m^3 additional volume. Meanwhile, the depression areas surrounding the central dome were observed with a depth between 0.5 and 4 m. The amount of material deposited on the volcano's summit was identified with a total volume of 2.93 x 10^6 m^3. This remaining deposited volume could be a potential lahar in the future. The ability to measure spatial and time-series of the lava dome changes from SfM-UAV, therefore, provides effective, detailed, and sometimes sole means of observing and quantifying dome surface emplacement in the period of before, during and after eruptions.

1. INTRODUCTION

Mount Agung (Bali, Indonesia) erupted for one and half years in 2017-2019. The intensive explosions and effusions occurred between November 21, 2017, and January 24, 2018, which were followed by smaller infrequent eruptions in the intermittent period until June 13, 2019, (Syahbana et al., 2019). During these periods of crisis, we have investigated the lava dome emplacement through five UAV campaigns (Andaru et al., 2021), i.e., three epochs before the eruption (October 19–21, 2017; the days are named "T1", "T2", and "T3", respectively), one epoch during the intensive eruption (Dec 16, 2017: "T4"), and the rest after the intermittent period (July 6, 2019: "T5"). According to the results, we have estimated that the lava dome had grown vertically by 126 m and had reached a volume of 26.8 million m^3 during the intense eruption. Furthermore, its surface had continued growing with surface uplifting up to 52 m during the intermittent period with an additional lava volume of 9.5 million m^3.

The last eruption of the Agung eruptive crisis, which lasted from 2017 to 2019, happened on June 13, 2019. Following that, the activity associated with the Mt. Agung explosions and effusions was deemed to have ended. At this point, the lava dome had grown to nearly one-third of the crater wall height, with a total lava volume of around 36 × 10^6 m^3 (Andaru et al., 2021). These decreasing intensities in seismicity and the relatively stable deformation inside the volcano (inferred from the field data analysis) thus led to lowering the Volcano Alert Level (VAL) to Level II on July 16, 2020 (ESDM, 2020).

In this work, we present a detailed account of the dome changes in terms of domes' growth and morphological features based on visual observations and image analysis associated with its lowered VAL. We discuss the impact of the eruptions on the landscape and calculate the remaining deposited lahar on the summit. The analysis involves the image datasets that had been collected in the intermittent period (T5) and the newest image dataset that was obtained in the decreasing alert level (July 16, 2020: "T6"). These image datasets were remotely collected with a fixed-wing UAV platform, i.e., Buffalo FX-79, capturing the summit with a flight altitude of 3,600 m above sea level.

Our use of the UAV-SfM method to observe and quantify the dome emplacement is not new, indeed. Previous volcanological applications utilizing UAV-photogrammetry have been widely used, such as for investigating tectonic features (Bonali et al., 2019), stratigraphic studies (Smith and Maxwell, 2021), assessments of dome-collapse and inflation volumes (Andaru and Rau, 2019; Zorn et al., 2020), and measuring surface deformation (Tibaldi et al., 2020). The UAVs' utilizations are increasingly used due to their flexibility in deploying the platforms, refinements of in-flight technology, ability to fly in thousand kilometers height, carrying many sensors, and increases in flight durations. The UAV-SfM products allow us to create detailed 3D models and high resolution of DSM including orthoimage that are useful for facilitating the identification of sub meter-scale features of dome morphology.

* Corresponding author, email: ruliandaru@ugm.ac.id

One year after the eruption crisis, this study aims to assess the post-eruptions ground surface deformations, identify the spreading of volcanic material eruption and the distribution of damaged structures, and investigate the affected hazard areas that have happened and may still happen. These mapped results should be acknowledged since they may help volcanologists and local governments mitigate further damage (Ybañez et al., 2021). For these purposes, apart from acquiring the UAV images on the summit, on the date of the T6 UAV campaign, we had acquired a large area of 282 km^2 that covered the mountain's slope and the downstream villages.

On the other hand, since the investigation was involved time-series UAV datasets, those datasets need to have a consistent reference frame and are geometrically co-registered. The purpose of this co-registration is mainly to minimize misalignment errors at the same areas captured on different dates (Cucchiaro et al., 2020). Regarding the measurements of well-distributed ground control points (GCPs) and accurate geotagged images that were not available for the entire datasets, there will lead to improper co-registration processes. This study, therefore, also highlights the co-registration strategy in order to minimize the errors of the generated DSMs.

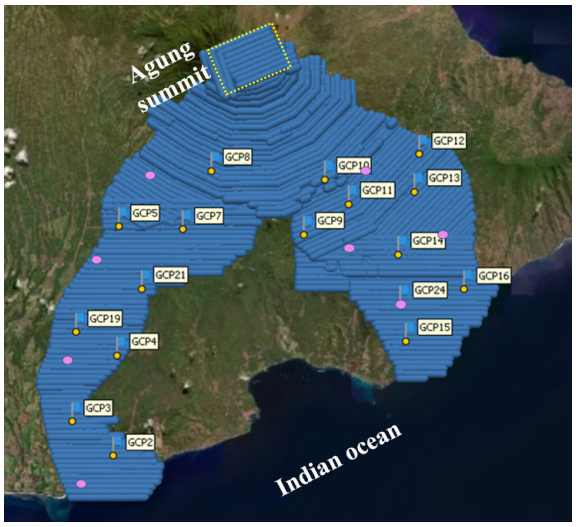

Figure 1. Distribution of GCPs (yellow dots) and CKPs (pink dotes) measured on the date of T6. The blue line illustrates the UAV trajectories of T6.

2. DATA AND METHODS

The datasets for Mt. Agung morphological changes analysis were obtained from six UAV campaigns in 2017–2020 (Table 1). Two UAV-fixed wing platforms (i.e., Buffalo FX-79 and Ai450) were used for the missions. Since this study focuses on the morphological changes one year after eruptions, the analysis only uses T5 and T6 datasets. The images on the date T5 covered an area of 33.2 km^2 (as depicted in a yellow rectangle in Fig 1) including the entire 0.67 km^2 of the crater. Meanwhile, the date T6 covered a larger area (from the summit to the southern of the volcano slopes towards the Indian ocean) with a total number of images of 24,950 (the flight trajectories are depicted in blue lines in Fig. 1).

The difficult and hazardous terrain on the summit did not make it possible to measure GCPs intended to create a reliable georeferencing. As shown in Fig 1, we had no on-site GCP measurement on the summit either on the date T5 or T6. Meanwhile, on the T6 dataset, we had measured 17 GCPs and eight check points (CKPs) that spread on the southern part of the volcano (their distributions are depicted in Fig 1). In addition, the UAV images acquired in both datasets were geotagged by using an on-board GNSSNAV system (~10 m in accuracy). These geotagged locations are taken into account during the GNSS-supported aerial triangulation (GNSS support AT) process. Consequently, a proper co-registration process was required to geo-reference those two datasets into a single reference frame.

2.1 Co-registration strategies

For co-registering T5 and T6 datasets, we applied an image-based co-registration (IBC) procedure to align both of the datasets under the GNSS-supported AT framework (Aicardi et al., 2016; Li et al., 2017). The IBC method itself is a co-registration strategy with a dependent AT procedure. Two image datasets (taken on different dates) were aligned together at the same scene; the one as the reference and the other one as the target. Hence, the corresponding tie-points between those two epochs were required. Since the T6 dataset has GCPs measurement, it was treated as the reference. The registration began by performing AT of the T6 dataset with the help of GCPs. The AT accuracy for this step was evaluated using the root mean square error (RMSE) of CKPs. To align T5 and T6 datasets, a subset overlapped region of both epochs was created (as shown in Fig. 2), followed by combining both images within the subset region into one scene. The image-based co-registration of T5-T6 datasets was then performed within this subset region. During this aligning, the resulted exterior orientation parameters (EOPs) of the T6 dataset were fixed in order to constrain the AT of the T5 dataset.

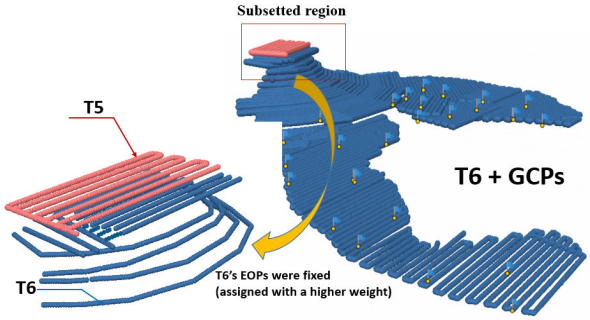

Figure 2. Subset region for co-registering T5 and T6 datasets

Epoch Time	Acquisition date	Days interval	UAV type	Number of images	Altitude (m)	Traveling distance (km)	Nominal spatial resolution (m)
T1	Oct, 19, 2017	-	Buffalo FX-79	95	4200	51	0.4
T2	Oct, 20, 2017	T1-T2: 1	Ai450	246	3400	34	0.2
T3	Oct, 21, 2017	T2-T3: 1	Buffalo FX-79	104	4000	51	0.3
T4	Dec, 16, 2017	T3-T4: 56	Ai450	100	3400	32	0.2
T5	July, 6, 2019	T4-T5: 567	Buffalo FX-79	640	4000	62	0.4
T6	July, 16, 2020	T5-T6: 376	Buffalo FX-79	24,950	600-3600	750	0.4

Table 1. UAV Surveys of the Mt. Agung lava dome

2.2 Photogrammetric processing

The UAV systems along with the SfM-MVS pipeline are capable for automatic generation of high spatial and temporal resolution dense point clouds. In this work, Metashape Pro software is adopted to accomplish these algorithms. Prior to generating dense point-clouds, pixel-based matching was performed to detect and match the feature points between image frames in different camera perspectives. Then, reconstructing the 3D scene structure as well as solving the intrinsic and extrinsic orientation parameters of the cameras through self-calibrating bundle adjustment (SCBA). Since both datasets were combined together into a single scene, thus the resulted SCBA of this scene (i.e., sparse point-clouds of those two datasets) had also been co-registered properly. After performing the SfM step, MVS algorithm was applied to generate dense point clouds. Furthermore, DTMs and orthoimages were generated from the entire set of well-registered dense point clouds.

2.3 Analysis of changes in morphology and land cover

For determining the lava dome emplacement quantitatively, we calculated the difference between T5 and T6 DSMs. Any changes in dome elevation and volume in one year after Mt. Agung eruptions can be estimated by subtracting the DSMs on those two datasets. Each pixel's vertical displacement on the lava dome's surface is represented by these quantitative values. For better visualization of the emplacements, including the lava dome growth during the eruption crisis, the entire time-series dome surfaces were integrated into a half-3D model. We also discovered the distribution of eruption material, which revealed the material losses and gain surrounding the crater. These calculations resulted in an estimation of the material deposition or erosion on the volcano's summit during the eruption. To accomplished it, DSM of Mt. Agung summit before eruption (i.e., T1) was incorporated. Hence, the T1-T4 datasets are required to be co-registered as well. However, since the lava dome surface underwent significant changes in the pre-, during, and post-eruptions, those four datasets cannot be co-registered through IBC due to the unavailability of performing tie points matching between epochs. Thus, we used cloud-to-cloud (C2C) matching technique with a coarse and fine registration process to complete the co-registration process. A detailed co-registration strategy of those datasets can be found in Andaru et al. (2021).

Furthermore, we also detect the changes in land cover after eruptions and recognize the area that was affected by the eruption material. For this purpose, the support vector machine (SVM) image classification algorithm was used (Kranjčić et al., 2019). The training areas representing the land cover classes (e.g., ground and erupted material) were determined in the T6 orthoimage using a region of interest (ROI) tool prior to image classification processing. These ROI training samples were then used to classify the images to produce land cover maps after the eruption.

3. RESULTS AND DISCUSSIONS

3.1 Co-registered of DSMs and orthoimages

Through IBC and cloud matching co-registration strategies, we have obtained proper co-registered point clouds and DSMs. The validity of aerial triangulation accuracy of the T6 dataset (as the first step in the IBC process) was evaluated using RMSE of CKPs during SCBA. It yielded horizontal and vertical RMSEs of 0.38 m and 0.47 m, respectively. In the meantime, the MVS algorithm would create a full 3D scene reconstruction and increase the density of the point clouds. Furthermore, the DSMs were created by interpolating the generated dense point clouds with a spatial resolution of 0.4 m. The resulted DSMs of six time-series Mt. Agung lava dome were illustrated in Fig 3. In the end, the orthoimages can be produced by rectifying the original UAV images with the help of the DSMs as shown in Fig 3.

The validity of the co-registration of T5 and T6 and the generated DSMs were evaluated by comparing the elevations of the surface models at several unchanged areas. It achieved a vertical RMSE of 0.58 m, which is about one and a half pixels of UAV image spatial resolution. The interpretation of both DSMs reveals that the dome surfaces have a solid crust and did not present any significant changes in shape. The depression areas in the central dome that was identified on T5 can be still found on the date T6 (as depicted in inset pictures of Fig 3a). Moreover, the lava material on both datasets had remained and accumulated near the dome edge. Analysis of the two series orthoimages also indicates that the crater surface's morphology was remarkably unchanged—the dome presents rough surfaces that resemble small stones and sand. However, the central dome of T6 has a smoother surface than that of T5, indicating that it contains a lot of sand material.

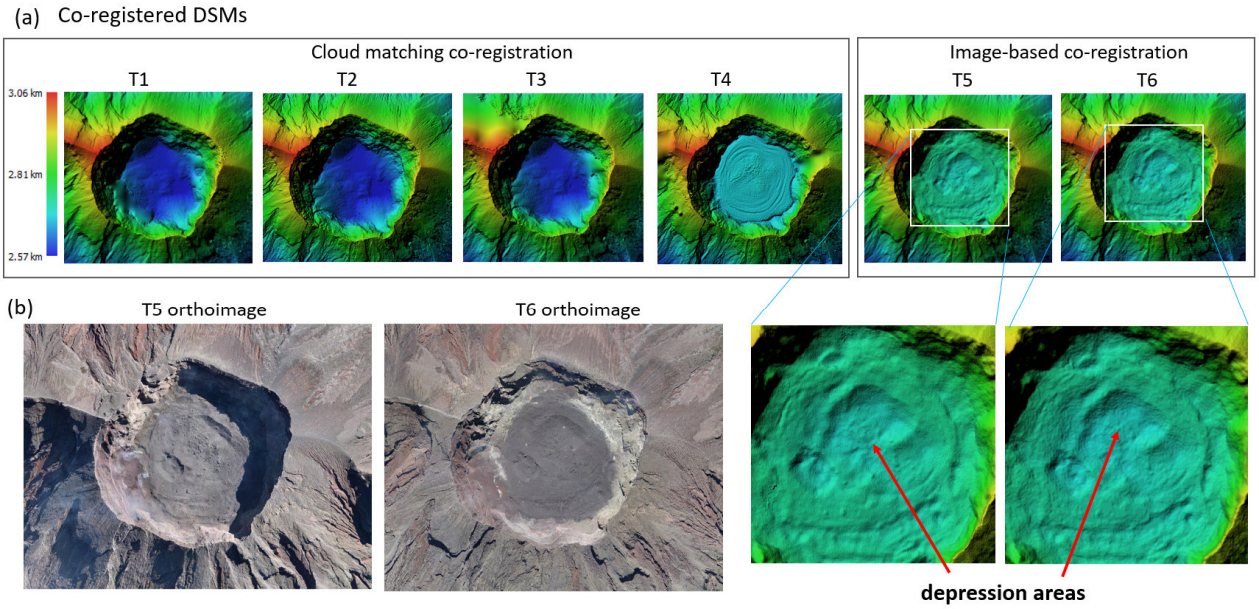

Figure 3. (a) Co-registered of six time-series DSMs. (b) Orthoimages of T5 and T6.

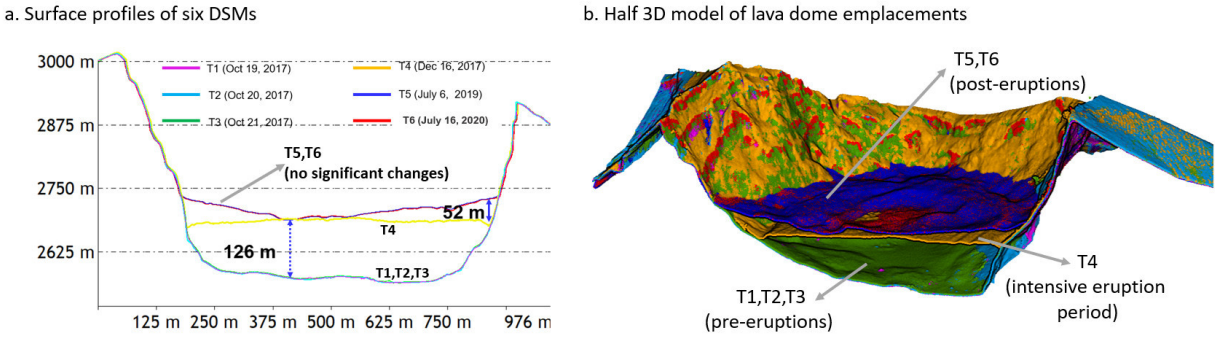

Figure 4. (a) Surface profiles of the vertical lava dome emplacements of the six datasets. (b) Half 3D model of lava dome emplacement over the six datasets.

3.2 Morphological changes

For a detailed investigation of the dome morphological changes, particularly in the estimation of vertical movement, surface profiles between two DSMs of T5 and T6 were created. The general expression based on these surface profiles reveals that the morphological lava dome is relatively stable. There were no significant surface changes or vertical displacements over dome surface (as depicted in the surface profiles and half 3D model in Fig 4a and b)—the surface profiles between T5 and T6 are closer and more consistent. The surface profiles of T5 and T6 are depicted as blue and red lines in Fig. 4a, respectively. It implies that no significant magma pressure accumulation occurred inside the dome one year after the eruption. Meanwhile, for better tracking the growth of the Mt. Agung lava dome, the surface profiles also incorporate the DSMs on the date T1-T4. As we have mentioned in our previous study, the lava dome grew significantly during the intensive eruptions period with a maximal vertical displacement of 126 m (as depicted in the yellow line in Fig 4a). The results also reveal that in the intermittent period, the lava dome still grew and reached a maximal uplift of approximately 52 m. According to the surface profile shown in Fig. 4a, by July 2020, the lava dome now has reached approximately one-third of the tallest crater wall height, with a total volume of 36.47 x 10^6 m^3.

The morphological changes were further assessed by using the generated DSMs and their differences to support quantitative analysis of the changes in geometric shape and depth. Fig. 5a provides the spatial information of these DSMs differences. This information reveals that the vertical depth and morphological changes illustrate the deformation of the lava dome surface. The light blue to dark blue indicates the dome growth, while the light red to dark red denotes the dome depression. Meanwhile, the beige color indicates the unchanged areas.

According to the results, we found a small-scale growth in the central dome (as depicted in the largest light blue regions in Fig 5a), increasing the dome height up to 2 m. This growth inflates the central dome with a volume of 45,950 m^3. Meanwhile, the local depression areas were observed surrounding the central dome with a depth between 0.5 and 4 m (depicted in the light to dark red color in Fig 5a). These depression areas deflate the dome surface with a volume of 30,383 m^3. We have also observed the growth of a new lava lake (e.g., compound lava) with an area of 9,166 m^2 in the southeast of the dome edge (depicted in the blue region in Fig 5a,b, and c). For detailed measurement of the dome and lava lake growth, a

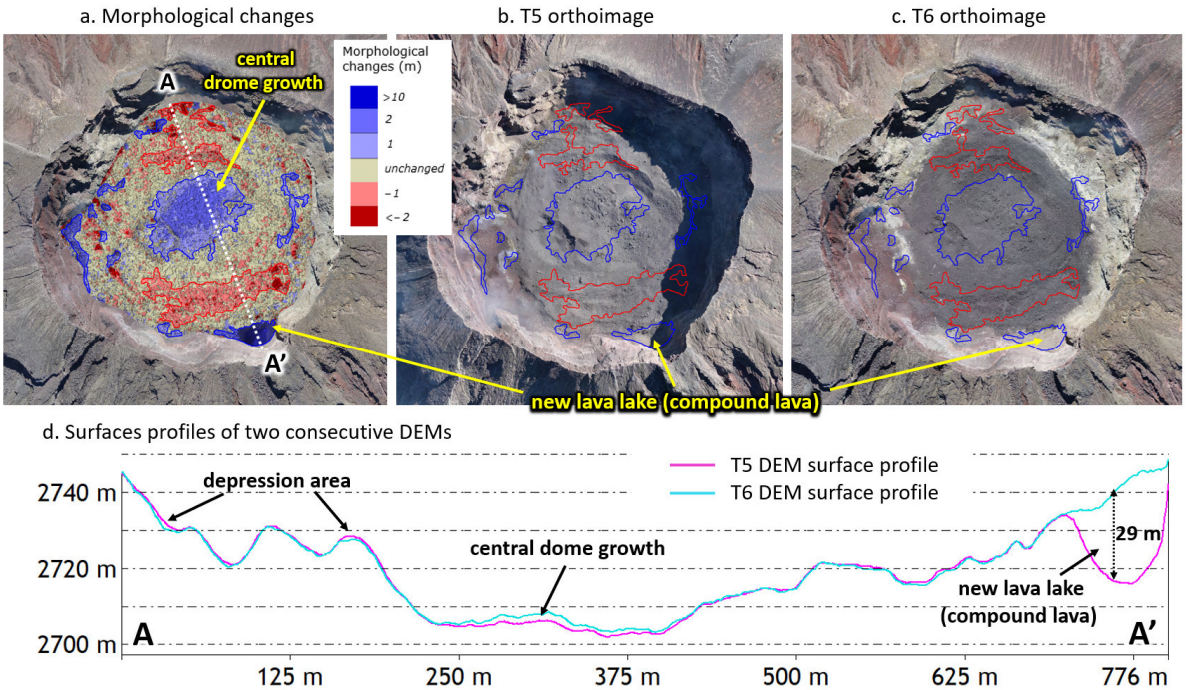

Figure 5. (a) Changes in morphology between T5 and T6 DTMs (exhibiting dome growth and the depression areas. (b) The T5 orthophoto and (c) T6 orthophoto. (d) Surface profiles of the T5 and T6 DSMs.

cross-sectional line of DSMs of T5 and T6 was created throughout the central dome to the edge (depicted as white dots line of A-A' in Fig. 5a). It reveals that the new lava lake has heights of up to 29 m, as measured in the surface profiles in Fig 5d). From volume calculation between two surfaces (i.e., T5 and T6 DSMs), it was estimated that this lava lake translated to a 79,623 m^3 deposition volume.

3.3 Changes in land cover and the deposited material after the eruptions

To detect the changes in the land cover after the eruptions and recognize the area that was affected by material eruptions, we used the orthoimage of T6. The orthoimage on this date covered the southern part of the mountain toward the downstream villages with an area of 282 km^2 (as shown in Fig. 6). The final identification of areas that were affected by the material eruption (through SVM algorithm and manual refinement) is overlaid in the T6 orthoimage. According to this result, the material eruptions were identified spreads and affect areas up to 2.2 km from the Agung summit with an area of approximately 11.2 km^2 (depicted in light-brown regions in Fig. 6). As identified, the lahars flew and extended by approximately 11 km along the existed valley or river which originated from the deposited material on the upstream. These lahars partly damaged some roads and bridges' constructions that connect several villages in the downslope areas (the locations are illustrated in the inset pictures of Fig. 6).

Since the DSMs of pre-eruptions are available in this study, there has been a chance to estimate the remaining deposited material eruption surrounding the summit. This volume could be argued to represent the actual amount of material that was deposited during the eruptions, making it a possible lahar in the future (Andaru et al., 2021). To estimate this value, the DSMs between T1 and T6 were subtracted in order to determine the height difference as an identifier of these depositions. According to the DSMs difference, it reveals that the volume of deposited material on the volcano's summit was 2.93 x 10^6 m^3 with respect to the overlapped areas of those two DSMs (depicted in Fig. 7 with area of 7.43 km^2). The figure illustrates the surface changes on the edifice slopes, where the blue and red areas indicate areas

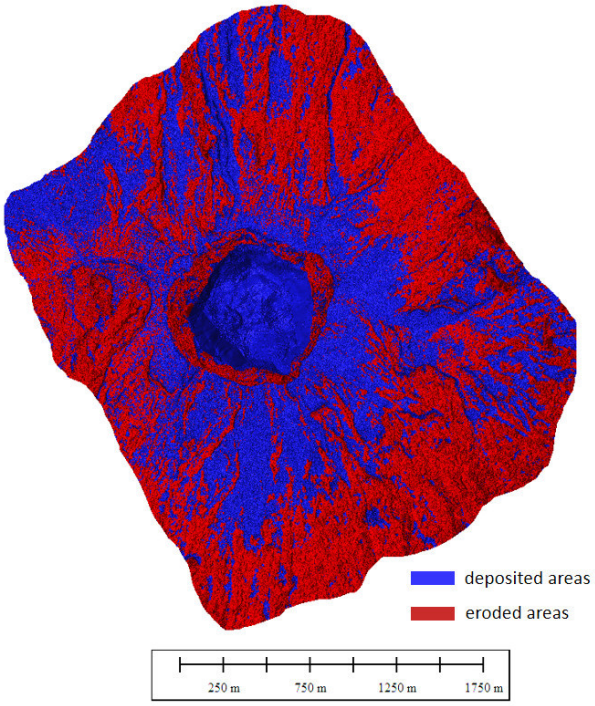

Figure 6. The DSMs difference between T1 and T6 over the overlapped areas of those two DSMs. The remaining deposited material eruptions are depicted as blue regions.

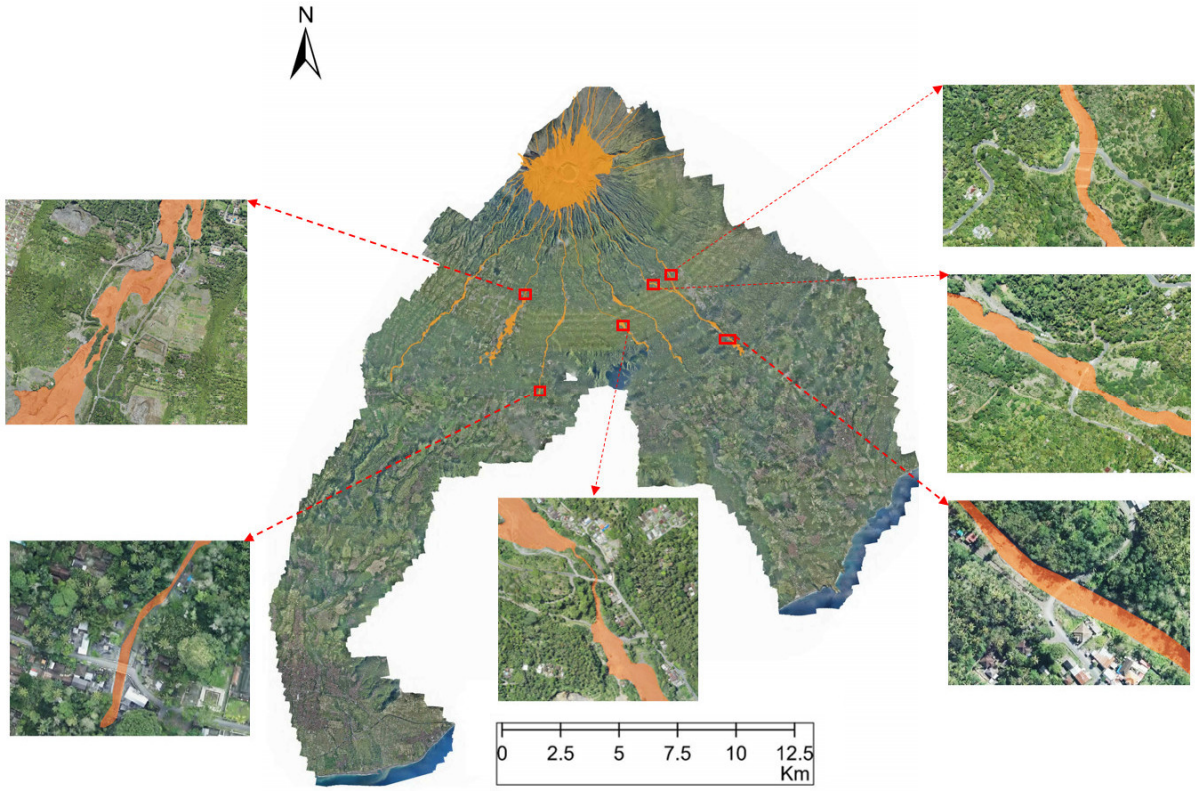

Figure 7. The affected areas of material eruption (overlaid on T6 orthoimage). Lahars hazard reportedly destroyed some roads and bridge.

of material gain (deposition) and loss (erosion), respectively. These deposited materials altered the elevation and profiles of the existing ravines, which posing a serious risk for secondary hazards (i.e., lahars; in tropical regions) (Calder et al., 2015).

4. CONCLUSIONS

This work demonstrates a potential method of detecting lava dome emplacement and the morphological changes with a photogrammetric method by utilizing UAV images. The UAV photogrammetry method makes it possible to produce a high resolution of DSM and orthoimages, facilitating the identification of sub-meter-scale feature changes of dome morphology. Six time-series UAV datasets (i.e., T1-T6) were involved in recognizing the dome growth and the morphological changes and tracking the changes through time.

One year after the 2017-2019 Mt. Agung eruptions, the post-eruption lava dome emplacement was investigated through the DSMs and orthoimages of T5 and T6 datasets. The results show that there were neither considerable surface displacements inside the dome nor changes in its surface texture, which mean that the Mt. Agung lava dome had remained stable for that period of time. These results are in accordance with the moment of the VAL decline to Level II, when was also declared on the same date of UAV acquisition (i.e., T6).

Meanwhile, although the dome had considerably remained stable, we observed a small-scale growth that uplifted the surface on the central dome and the growth of a new lava lake on the dome edge. In addition, a considerable amount of deposited material eruptions on the volcano's summit was still identified, which could be potential lahars in the future. Furthermore, we prove that the UAV-photogrammetry is available to map the whole volcano region (which covers the summit region toward the downslope area), providing practical and effective way (in terms of data collection) with acceptable accuracy. The UAV products can be useful for detailed hazard assessment, such as for identifying the dome growth and the impact of the eruptions over the landscape as well as estimating the deposited material eruptions that may cause future lahars.

ACKNOWLEDGEMENTS

We would like to thank the Ministry of Science and Technology (MOST) Taiwan for providing financial supports and the Indonesian Center for Volcanology and Geological Hazard Mitigation for supporting the supplementary of UAV images. We are also grateful to Total Geo Survey and TomCat aeromodelling for providing UAV maintenance and data collection service. Additionally, we acknowledge Iwan Trisnawan, Rio Andi, and Rahmat Muslih for contributing to the field observations. Finally, we would like to appreciate all the reviewers giving their constructive suggestions to improve the article.

REFERENCES

Aicardi, I., Nyapwere, N., Nex, F., Gerke, M., Lingua, A.M., Koeva, M.N., 2016. Co-Registration of Multitemporal Uav Image Datasets for Monitoring Applications: A New Approach. *ISPRS - International Archives of the Photogrammetry, Remote Sensing and Spatial Information Sciences*. XLI-B1, 757-763.

Andaru, R., Rau, J.-Y., Syahbana, D.K., Prayoga, A.S., Purnamasari, H.D., 2021. The use of UAV remote sensing for observing lava dome emplacement and areas of potential lahar hazards: An example from the 2017–2019 eruption crisis at Mount Agung in Bali. *Journal of Volcanology and Geothermal Research*. 415, 107255-107276.

Andaru, R., Rau, J.Y., 2019. Lava dome changes detection at Agung mountain during high level of volcanic activity using uav photogrammetry. *ISPRS - International Archives of the Photogrammetry, Remote Sensing and Spatial Information Sciences*. XLII-2/W13, 173-179.

Bonali, F.L., Tibaldi, A., Marchese, F., Fallati, L., Russo, E., Corselli, C., Savini, A., 2019. UAV-based surveying in volcano-tectonics: An example from the Iceland rift. *Journal of Structural Geology*. 121, 46-64.

Calder, E.S., Lavallée, Y., Kendrick, J.E., Bernstein, M. 2015. *Chapter 18 - Lava Dome Eruptions*. Academic Press, Amsterdam.

Cucchiaro, S., Maset, E., Cavalli, M., Crema, S., Marchi, L., Beinat, A., Cazorzi, F., 2020. How does co-registration affect geomorphic change estimates in multi-temporal surveys? *GIScience & Remote Sensing*. 57*(5)*, 611-632.

ESDM, 2020. Press Release : Update on the Volcanic Activity of Mount Agung (16 July 2020). https://magma.esdm.go.id/v1/press-release?page=3#, (accessed 20 July, 2020)

Kranjčić, N., Medak, D., Župan, R., Rezo, M., 2019. Support Vector Machine Accuracy Assessment for Extracting Green Urban Areas in Towns. *Remote Sensing*. 11*(6)*.

Li, W., Sun, K., Li, D., Bai, T., Sui, H., 2017. A New Approach to Performing Bundle Adjustment for Time Series UAV Images 3D Building Change Detection. *Remote Sensing*. 9*(6)*.

Smith, Z.D., Maxwell, D.J., 2021. Constructing vertical measurement logs using UAV-based photogrammetry: Applications for multiscale high-resolution analysis of coarse-grained volcaniclastic stratigraphy. *Journal of Volcanology and Geothermal Research*. 409, 107122.

Syahbana, D., Kasbani, K., Suantika, G., Prambada, O., Andreas, A., Saing, U., Kunrat, S., Andreastuti, S., Martanto, M., Kriswati, E., Suparman, Y., Humaida, H., Ogburn, S., Kelly, P., Wellik, J., Wright, H., Pesicek, J., Wessels, R., Kern, C., Lisowski, M., Diefenbach, A., Poland, M., Beauducel, F., Pallister, J., Vaughan, R., Lowenstern, J., 2019. The 2017-19 activity at Mount Agung in Bali (Indonesia): Intense unrest, monitoring, crisis response, evacuation, and eruption. *Scientific Reports*. 9*(8848)*.

Tibaldi, A., Bonali, F.L., Russo, E., Fallati, L., 2020. Surface deformation and strike-slip faulting controlled by dyking and host rock lithology: A compendium from the Krafla Rift, Iceland. *Journal of Volcanology and Geothermal Research*. 395, 106835.

Ybañez, R.L., Ybañez, A.A.B., Lagmay, A.M.F.A., Aurelio, M.A., 2021. Imaging ground surface deformations in post-disaster settings via small UAVs. *Geoscience Letters*. 8*(1)*, 23.

Zorn, E.U., Walter, T.R., Johnson, J.B., Mania, R., 2020. UAS-based tracking of the Santiaguito Lava Dome, Guatemala. *Scientific Reports*. 10*(1)*, 8644.